The DC Arc Fault Detection Method Taken Advantage of WT and MFE

Zhendong Yin, Li Wang, Yaojia Zhang, Yang Gao, Shanshui Yang
College of Automation
Nanjing University of Aeronautics and Astronautics
Nanjing, China
zd_yin@nuaa.edu.cn

***Abstract*—Compared with AC arc faults, there isn't zero-crossing points in the current waveform when the DC arc faults occur. Dc arc fault brings great harm to the safe operation of power supply system. Wavelet transform (WT) is suitable for analyzing non-stationary signal, and multi-scale fuzzy entropy (MFE) is of excellent performance in detecting the uncertainty and complexity of the signal. The random fluctuation and uncertainty of current will be greatly enhanced when arc faults occur. This paper aims to elevate the property of detection of dc arc faults, WT and MFE are utilized to construct the fault features. Least squares support vector machine (LSSVM) is employed to be as the classifier to make the detection of dc arc faults. The result of the experiment shows the availability of the method this paper proposed.**

Keywords-DC arc; WT; MFE; LSSVM; fault detection

I. INTRODUCTION

With the development of the technology of power electronics, dc power supply system is increasingly used in aerospace, ships, electric cars, trains and smart power grid and other fields [1][2]. Dc power supply system does not have eddy current loss, nor need to carry out phase and frequency tracking. So that the transmission of power is more efficiency [3]. Within the dc power supply system, dc arc faults often occur under the conditions of loose metal joints, damaged insulation, open circuit or grounded short circuit. Arc is a phenomenon of electric discharge between conductors which breaks through the air. It is usually accompanied by high temperature and strong light, and the fault range is easy to expand rapidly. Thus, it will damage the insulated wire and ignite the surrounding combustible, and there is most likely be a fire or even an explosion. Different from the ac arc faults, there is not cross the zero points when the dc arc faults occur, and it is difficult to extinguish by itself after generation.

DC arc faults contain two types: parallel dc arc fault and series dc arc fault. When the parallel arc faults occur in the system, the working current is generally higher than that during normal. At this time, the over-current protection module insided the system is able to eliminate the parallel arc fault in time and to safeguard the system. However, when the series arc fault occurs, the current value is relatively small due to the limitation of the load, which generally less than 35A. It is difficult for the over-current protection to achieve the safeguard in this case [4]. Therefore, in order to make the dc power supply system operate safely and stably, it is necessary to investigate the series dc arc faults' detection strategy.

Through detecting the sound, light, heat, electromagnetic radiation and other signals generated by arc faults, [5-8] realize the prevention of the circuit. However, these methods are limited by the placement position of the sensor which are difficult to be widely used.

Nowadays, Arc fault detection methods on the strength of the circuit current are one of the main detection methods. [9] takes the current drop as a sign of dc arc precursor, which can play a protective role immediately after the air gap is formed. [10] detects the occurrence of an arc fault by determining whether the maximum or minimum current exceeds a set threshold. [11] used the instantaneous drop in current as a criterion for whether an arc occurred. In the opinions of [12][13], the frequency band range of 0.1~100khz in current contains more information of dc arc faults. [14] uses the method based on frequency domain information to detect arc faults in the photovoltaic system, which is able to distinguish the arc state from the normal working state effectively. By using the current standard deviation, peak-to-peak value and harmonic power in the range of 1-100khz frequency band as the fault characteristics [15], the dc arc faults detection is realized by using the mahalanobis distance method as the classifier. In [16], the maximum value of current signal, the variance of wavelet coefficient is regarded as the fault characteristics, and the mixed criteria are specified to realize dc arc fault detection in photovoltaic system. The working conditions such as voltage, current and load properties often change in the dc power supply system. The series dc arc faults detection method based on time-frequency information is greatly affected by the working conditions and prone to misjudgment [17].

Compared with traditional Fourier analysis, WT has better time-frequency localization ability and multi-resolution characteristics, and which is of the ability to analysis the local features of time series in both time domain and frequency domain. And WT is of stronger feature extraction performance [18-20]. The ac component of current contains a large number of abrupt and non-stationary components. WT is of obvious advantages in processing non-stationary signal.

Fuzzy entropy (FE) is of the capacity to measure the probability of the generation of new patterns in the phase space when the dimension of time series changes and represents the

978-1-7281-0860-5/19/$31.00 ©2019 IEEE

complexity of the data [21]. The FE is not only independent of the length of data compared with sample entropy, but also has better relative consistency. And the data required for the calculation of FE is shorter than sample entropy. Compared with the ac component of current during normal operations, the ac component of current during arc conditions contains a large mass of random harmonic and the complexity of the current signal is higher. Therefore, FE can be considered as the fault features of dc series arc faults detection. Under different scales, the complexity of ac component of current can be measured in a more comprehensive way [22], and the exploration of the deeper fault information hidden in different scales of the time series is able to be realized. This paper, MFE is applied to make the fault detection of series dc arc faults come true for the first time.

For solving the issue that the serial dc arc fault detection method based on time-frequency information is easy to be interfered by working conditions, this paper, a series dc arc fault detection method taken advantage of WT and MFE is put forward. Firstly, the current signal can be decomposed into multi-layer signals by WT and remain the first layer of the component which contains most information of arc faults. Therefore, the interference of the low-frequency components can be filtered out. Then, the MFE of filtered current signal can be calculated to construct the high dimensional fault features. Finally, least squares support vector machines (LSSVM) is applied to realize the serial dc arc fault detection. The experimental results indicate that the effectiveness of the proposed method.

II. Research Platform of Arc Faults and Data Collection

A. Arc Faults Generator

The arc faults generator is an important part of the research platform for arc faults detection. Figure 1 is the structure diagram of the device. The arc faults generator meets the standards UL1699B and GB14287. The dynamic side is controlled by a stepping motor to achieve speed of arc controllable, and maximum distance of the copper rod and carbon rod is 100mm and the motion accuracy is 10μm.

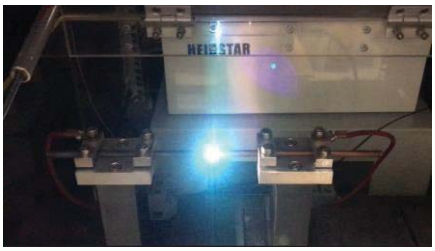

Figure 1. Structure diagram of arc generator

B. Research Platform of Arc Faults

This paper builds the research platform of arc faults in order to research the features of DC arc, the schematic diagram of arc fault research platform shown in Figure 2. The computer controls the realization of the automatically injection of arc fault, and which is bale to remotely control the electric arc generator through serial port.

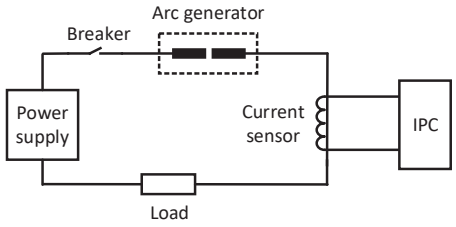

Figure 2. The schematic diagram of arc fault research platform

C. Data Collection

For investigate the features of dc series arc faults, four kinds of resistive loads are adopted: 5Ω、10Ω、15Ω and 20Ω. In each load condition, experiments were carried out with different current levels to collect current data. In each current level condition, 12 groups of data were collected, among which 4 groups are collected during normal operations and 8 groups were collected during arc faults conditions. The operating conditions under different loads are presented in Table I.

The number of data sets collected during normal operations and during arc faults conditions is 336. 168 sets of data were taken as the training data set, and the other 168 sets of data were taken as the test data sets.

TABLE I. THE OPERATING CONDITIONS UNDER DIFFERENT LOADS

Output voltage (V)		60-80	60-154	60-227	60-299
Output current (A)		10-14	5.3-14	3.6-14	2.7-14
Sampling type		Regulate Circuit			
Load	***Type***	Resistor	Resistor	Resistor	Resistor
	Size	5Ω	10Ω	15Ω	20Ω
Electrode materials	***cathode***	Copper	Copper	Copper	Copper
	anode	Carbon	Carbon	Carbon	Carbon
condition		Normal and Arc			
The number of classes		48	96	96	96

Figure 3 shows the waveform of ac component of current, which is under the condition of 10 Ω and 8A. The waveform before 0.05s represents the normal operations, and the waveform after 0.05s represents the arc faults conditions. It can be seen that noise current ac component and wave amplitude during arc faults conditions are bigger than that during normal operations.

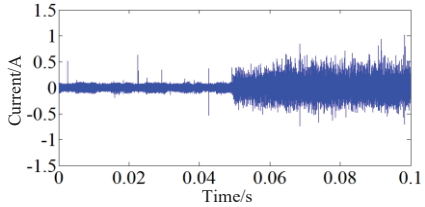

Figure 3. The waveform of ac component of current duiring normal operations and arc faults conditions

III. The Extraction of Fault Features

When dc serial arc faults occur, Ac component of current will be doped with a large number harmonic. This paper, the ac

component of current is decomposed into multilayer signals by WT firstly, and the component of first layer is preserve. Then, the high dimensional fault features obtained by MFE is used as the input of LSSVM.

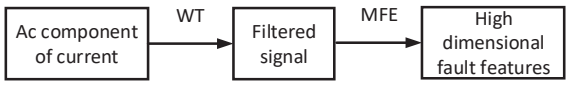

Figure 4. The Flow diagram of the extraction of high dimensional feature

A. WT

By using orthogonal wavelet basis, the WT based on multiresolution theory is able to decompose signal into several components in different scales. The basic principle of WT is able to be describe as follows

$$C_\psi = \int_R \frac{\left|\hat{\psi}(\omega)\right|^2}{|\omega|} d\omega < \infty \tag{1}$$

By stretching and translation, the generation function $\psi(t)$ is obtained

$$\psi_{a,b} = \frac{1}{\sqrt{|a|}} \psi(\frac{t-b}{a}) \tag{2}$$

where, $a,b \in R$ and $a \neq 0$

The continuous WT of the signal $f(t)$ is

$$W_f(a,b) = \left\langle f, \psi_{a,b} \right\rangle = |a|^{-\frac{1}{2}} \int_R f(t) \psi(\frac{t-b}{a}) dt \tag{3}$$

Then the inverse transformation is

$$f(t) = \frac{1}{C_\psi} \int_{-\infty}^{\infty} \int_{-\infty}^{\infty} \frac{1}{a^2} W_f(a,b) \psi(\frac{t-b}{a}) da db \tag{4}$$

The above is the principle of continuous WT, but discrete wavelet transform is more widely used in practice. In Discrete WT, the scale parameter a and the translation parameter b are discretized: $a = a_0^m (m \in Z, a_0 > 1)$, $b = nb_0 a_0^n (n \in Z, b_0 > 0)$. The principle of discrete WT is as follows

$$\psi_{m,n}(t) = \frac{1}{\sqrt{a_0^m}} \psi(\frac{t - nb_0 a_0^m}{a_0^m}) = a_0^{-m/2} \psi(a_0^{-m} t - nb_0) \tag{5}$$

The inverse transformation of the discrete WT is

$$\left\langle f, \psi_{m,n} \right\rangle = \int_{-\infty}^{\infty} f(t) \psi_{m,n}(t) dt = a_0^{-m/2} \int_{-\infty}^{\infty} f(t) \psi(a_0^{-m} t - nb_0) dt \tag{6}$$

If a_0 and b_0 in equation (6) are set as 2 and 1 respectively, then the discrete WT in this case is binary discrete WT, which also namely orthogonal discrete WT. The WT in this paper refers to discrete WT.

This paper, db3 wavelet is used for the multi-layer decomposition of ac component of current. *S* is the original signal, A is the components of low-frequency, and *D* is the components of the high-frequency. The high-frequency components contains more arc noise of the original signal, and the component of low-frequency includes more trend terms of the original signal.

B. FE

In FE, similarity measurement formula is blurred by exponential function. And in this way, the measurement formula is able to change smoothly and continuously. By calculating the mean value, the influence of baseline drift is able to be removed. The vectors' similarity is on account of the fuzzy function, instead of being determined by absolute amplitude difference. Finally, the similarity measurement is fuzzified. The description of FE is as shown below

For the time series $\{u(i), i = 1,2,\cdots,N\}$, the m-dimensional vectors are obtained

$$\begin{aligned} X_i^m &= \{u(i), u(i+1), \cdots, x(i+m-1)\} - u_0(i) \\ & i = 1,2,\cdots,N-m+1 \end{aligned} \tag{7}$$

where, X_i^m represents the m continuous u_0(i) from the *i*th point. And in X_i^m, the mean of u_0(i) is removed.

$$u_0(i) = \frac{1}{m} \sum_{j=0}^{m-1} u(i+j) \tag{8}$$

$d[X_i^m, X_j^m]$ represent the distance between X_i^m and X_j^m, which is the maximum value of the difference between the corresponding elements.

$$\begin{aligned} d_{ij}^m = d[X_i^m, X_j^m] = \max_{k \in (0,m-1)} \{ & |(u(i+k) \\ & - u_0(i)) - (u(j+k) - u_0(j))| \} \\ & i, j = 1,2,\cdots,N-m, i \neq j \end{aligned} \tag{9}$$

The similarity of vector X_i^m and X_j^m is defined by fuzzy function $\mu(d_{ij}^m, n, r)$

$$D_{ij}^m = \mu(d_{ij}^m, n, r) = e^{-(d_{ij}^m / r)^n} \tag{10}$$

where, the fuzzy function $\mu(d_{ij}^m, n, r)$ is the exponential function. *n* is the gradient and *r* is the width of its boundary.

Defining that

$$\phi^m(n,r) = \frac{1}{N-m} \sum_{i=1}^{N-m} (\frac{1}{N-m-1} \sum_{\substack{j=1 \\ i \neq j}}^{N-m} D_{ij}^m) \tag{11}$$

Analogously

$$\phi^{m+1}(n,r) = \frac{1}{N-m} \sum_{i=1}^{N-m} (\frac{1}{N-m-1} \sum_{\substack{j=1 \\ i \neq j}}^{N-m} D_{ij}^{m+1}) \tag{12}$$

FE is defined as

$$\begin{aligned} FuzzyEn(m,n,r) = \lim_{N \to \infty} [& \ln \phi^m(n,r) \\ & - \ln \phi^{m+1}(n,r)] \end{aligned} \tag{13}$$

There are 3 parameters in FE: *r* is the similarity tolerance ; *n* is the similarity tolerance boundary's gradient; m is the embedded dimension . which represent the width of fuzzy function's boundary. Generally, *r* fall in between of 0.1 and

0.25 times of the standard deviation of the original data. Based on the recommendation of paper [24], r is times of the original data's standard deviation. n is set to 2, and m is set to 2.

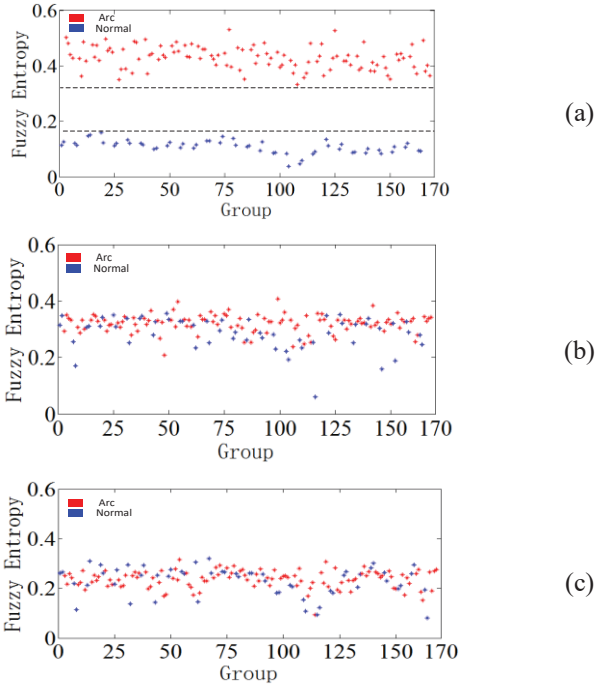

Figure 5. The FE (a) D_1; (b) D_2; (c) D_3;

Taking 10 Ω load as an example, firstly, the current data of 48 groups were decomposed into 6 components by WT. Then, the FE of each component is calculated. Due to the limitations of the space of the paper, only the FE of first three components are given here, and the results are shown in Figure 5.

Only the FE of the first component D_1 in Figure 5 (a) can distinguish the arc faults conditions from the normal operations. The results show that the FE of D_1 is suitable for series dc arc faults detection.

The fuzzy entropy calculated by component D_2 and component D_3 cannot effectively distinguish the arc faults conditions from the normal operations. This also confirms that the characteristics of arc noise of the current are mainly concentrated in component D_1, and WT removes the information in the original signal that are not related to arc characteristic. Therefore, only the MFE of component $D1$ is calculated in the following part of this paper.

C. MFE

When calculating the FE at different scales, MFE is obtained. For example, the time series $\{u(i), i = 1,2,\cdots,N\}$, $\{y_i^{(\tau)}\}$ (the coarse granulation sequence) are able to be obtained.

$$y^{(\tau)} = \frac{1}{\tau}\sum_{i=(j-1)\tau+1}^{j\tau} u_i \quad j = 1,2,\cdots,[N/\tau] \tag{14}$$

where, $[N/\tau]$ represents the rounding of N/τ, τ is the time scale. u is broken into τ coarse grained vector series $\{y_i^{(\tau)}\}$ with the length $[N/\tau]$ when τ is bigger than 1.

Taking the situation when the load type is 10Ω as an example, the first 6 scales of MFE of the filtered current signal are shown in the Figure 6. Blue points represent the MFE value during normal operations, and red points represent the MFE value during the arc fault conditions. The MFE obtained in the first four scales are able to distinguish the normal operations and arc faults conditions obviously. Moreover, with the change of voltage, current and load, the degree of differentiation between arc faults conditions and normal operations is not weakened. Therefore, MFE is robust to the change of operating conditions.

When the scale is larger than 4, the MFE can no longer distinguish the arc faults conditions from the normal operations. Therefore, the MFE calculated at the first 4 scales is selected in as the feature vector for the serial dc arc faults detection later.

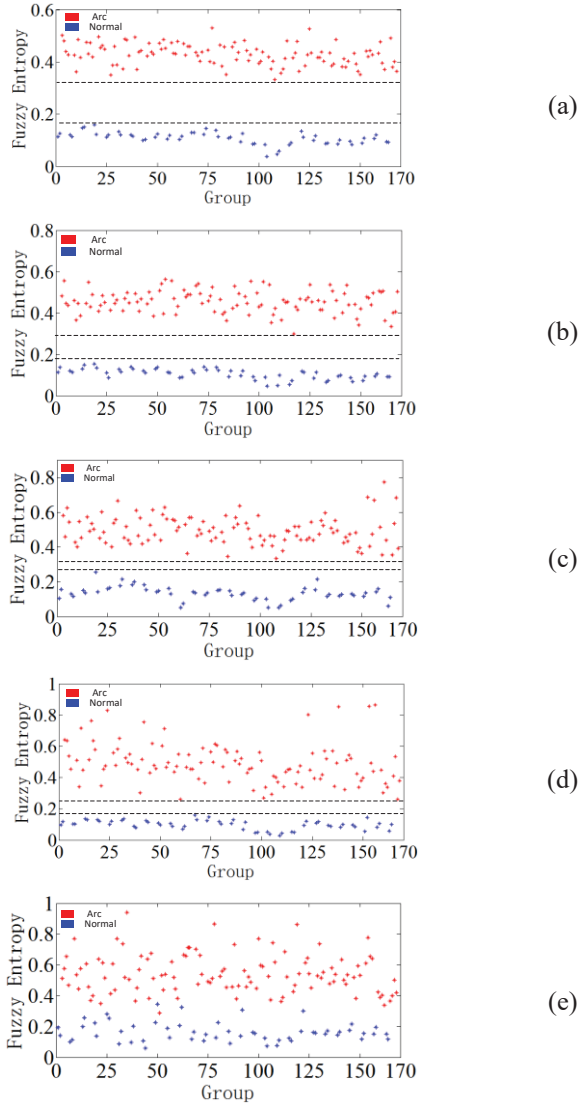

Figure 6. The fuzzy entropy of. (a) The 1th scale; (b) The 2th scale; (c) The 3th scale; (d) The 4th scale; (e) The 5th scale.

IV. ARC FAULTS DETECTION

A. LSSVM

In 1995, support vector machine (SVM) was firstly proposed by Vapnik [24]. The rationale of SVM is based on the statistical modeling theory. When the sample is small, the global optimal solution is able to be obtained. Moreover, SVM can not only estimate samples with high accuracy, but also has strong generalization ability based on structural risk minimization criterion. As an improved form of SVM, Least squares support vector machine (LSSVM) solves the solving linear equations problems instead of the convex quadratic programming problem. The operation time is greatly reduced. Specifically, the basic principles of LSSVM are as follow

$$\min_{\omega,b,\xi} J_{LS}(\omega,\xi)=\frac{1}{2\|\omega\|^2}+\frac{1}{2\gamma\sum_{i=1}^{N}\xi_i^2} \tag{15}$$

Taking the constrain condition into consideration

$$\begin{aligned} y_t[\omega^T\phi(x_i)+b]&=1-\xi_i \\ (i&=1,2,\cdots,N) \end{aligned} \tag{16}$$

In order to work out the optimization problem, lagrange function is constructed.

$$\begin{aligned} L_{LS}(\omega,b,\xi,\alpha)&=J_{LS}(\omega,\xi)- \\ &\sum_{i=1}^{N}\alpha_i\{y_i[\omega^T\phi(x_i)+b]-1+\xi_i\} \end{aligned} \tag{17}$$

where, Lagrange multiplier is α.

The linear equation is able to obtained by seeking the extreme of α_i、ξ、ω and b in (17) respectively.

$$\begin{bmatrix} o & Y^T \\ Y & ZZ^T+\gamma^{-1}I \end{bmatrix}\begin{bmatrix} b \\ a \end{bmatrix}=\begin{bmatrix} 0 \\ I \end{bmatrix} \tag{18}$$

where， $Z=[\varphi(x_1)^T y_1,\ \varphi(x_2)^T y_2,\ \cdots,\ \varphi(x_N)^T y_N]$; $Y=[y_1,\ y_2,\cdots,\ y_N]$; $I=[1,\ 1,\ \cdots,\ 1]^T$; $\xi=[\xi_1,\ \xi_2,\cdots,\ \xi_N]^T$; $\alpha=[\alpha_1,\ \cdots,\ \alpha_N]^T$.

Kernel function is defined as the form of $K(x_i,x_j)=\varphi(x_i)^T\varphi(x_j)$. In this paper and the Radial Basis Function is applied as the kernel function.

$$K(x_i,x_j)=\frac{\exp(-\|x_i-x_j\|^2)}{\sigma^2} \tag{19}$$

The parameter γ and σ^2 are of major influence on the performance of LSSVM. This paper, Cross-validation is utilized to select the parameters of SVM to improve the classification performance of LSSVM.

B. The Arc Faults Detection by LS-SVM

Before the detection of arc faults, LSSVM is trained by the training sets. Firstly, extracting the MFE of training set in Table I to construct high-dimensional fault features. Under normal operations, the labels of the fault features are set to 1, and under arc faults conditions, the labels of the fault features are set to -1. Then, cross-validation is applied to get the best parameters of LSSVM and the trained LSSVM model is obtained. The optimal parameters γ and σ^2 of LSSVM are 1.1721 and 6.7167 respectively. Then, the trained LSSVM was tested with test data sets, and the accuracy of arc faults detection was counted.

The comparison between the output labels by LSSVM and the original labels is shown in Figure 7, and the Table II is the detection results. As shown in Table II, only the 84th group of test sets is misclassified, and in this case, the 84th group of test sets during arc faults condition is identified as that normal operation. The total detection accuracy of the method proposed this paper is 99.4%, indicating that the method is of outstandingly detection peculiarity.

For the further verify the performance of the method proposed in this paper, a comparison test was designed. The method used for the comparison is based on time-frequency characteristics. The data in Table I were also used in the comparison test. The peak-to-peak value, standard deviation, average value and harmonic power were used as the fault characteristics, and LSSVM was utilized as the classifier. The optimal parameters γ and σ^2 of LSSVM obtained by cross-validation method are 1.1721 and 6.7167 respectively. Then, using trained LSSVM detects the test sets. In this case, the comparison between the output labels by LSSVM and the original labels is shown in Figure 8.

As shown in Table II, the number of the groups of test sets mistakenly detected by the method based on time-frequency features is 9. 4 groups during normal operations are identified as that arc faults conditions, and 5 groups of test sets during arc faults conditions are identified as the case during normal operations. The detection accuracy during normal operations is 90.47 %, and the detection accuracy during arc faults conditions is 96.03 %. The total detection accuracy based on time-frequency features is 94.04%.

Therefore, above analysis shows that the series dc arc fault detection method based on WT and MFE has better detection performance than that based on time-frequency features.

TABLE II. DIAGNOSIS PERFORMANCE

Method	**The method this paper proposed**		**Time-frequency domain analysis**	
State	***Normal***	***Arc***	***Normal***	***Arc***
The number of wrongly detected	84		69,86,92,114,118,134, 139,166,167	
Detection accuracy	100%	99.21%	90.47%	96.03%
	99.4%		94.04%	

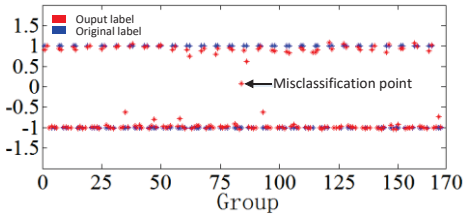

Figure 7. The detection performance of the method this paper proposed

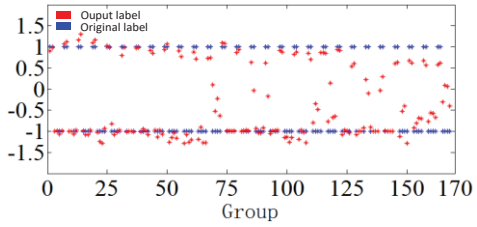

Figure 8. The detection performance of the method based on time-frequency features

V. CONCLUSIONS

Because of the randomness and instability of dc arc faults, A novel arc faults strategy taken advantage of WT and MFE is proposed to improve the performance of the detection of dc arc faults. First of all, in order to wipe out the noise in the signal, WT is employed to filter the current signal. And then, high-dimension features are constructed by utilized MFE. Finally, the LSSVM trained by high- dimension features are used to detect the dc arc faults. Experimental results indicate that the strategy this paper proposed is of better performance than the strategy based on time-frequency characteristics, and method this paper proposed is effective.

ACKNOWLEDGMENT

The authors appreciate the support of National Natural Science Foundation of China (Grant No.51877102).

REFERENCES

[1] J. A. Momoh and R. Button, "Design and analysis of aerospace DC arcing faults using fast fourier transformation and artificial neural network," *2003 IEEE Power Engineering Society General Meeting*, Toronto, Ont., 2003, pp. 788-793 Vol. 2.

[2] M. Naidu, T. J. Schoepf and S. Gopalakrishnan, "Arc fault detection scheme for 42-V automotive DC networks using current shunt," in *IEEE Transactions on Power Electronics*, vol. 21, no. 3, pp. 633-639, May 2006.

[3] Q. Hongxia, W. Chengshan, L. Shu, et al. “Discussion on the technology of intelligent micro-grid and flexible distribution system,” in *Power System Protection and Control*, 2016.

[4] R. F. Ammerman, T. Gammon, P. K. Sen and J. P. Nelson, "Dc arc models and incident energy calculations," *2009 Record of Conference Papers - Industry Applications Society 56th Annual Petroleum and Chemical Industry Conference*, Anaheim, CA, 2009, pp. 1-13.

[5] M. Goodman, "How ultrasound can detect electrical discharge non-invasively and help eliminate arc flash incidents," *2007 Electrical Insulation Conference and Electrical Manufacturing Expo*, Nashville, TN, 2007, pp. 247-252.

[6] S. Panetta, "Design of arc Flash protection system using solid state switch, photo detection, with parallel impedance," *2013 IEEE IAS Electrical Safety Workshop*, Dallas, TX, 2013, pp. 211-213.

[7] Q. Xiong, S. Ji, L. Zhu, L. Zhong and Y. Liu, "A Novel DC Arc Fault Detection Method Based on Electromagnetic Radiation Signal," in *IEEE Transactions on Plasma Science*, vol. 45, no. 3, pp. 472-478, March 2017.

[8] C. E. Restrepo, "Arc Fault Detection and Discrimination Methods," *Electrical Contacts - 2007 Proceedings of the 53rd IEEE Holm Conference on Electrical Contacts*, Pittsburgh, PA, 2007, pp. 115-122.

[9] S. Guo, J. Jones, and A. Dooley, “DC arc detection and prevention circuit and method,” U.S. Patent 6 683 766 B1, Jan. 27, 2004.

[10] M. Dargatz and M. Fornage, “Method and apparatus for detection and control of dc arc faults,” U.S. Patent 8 179 147 B2, May 15, 2012.

[11] X. Yao, L. Herrera, S. Ji, K. Zou and J. Wang, "Characteristic Study and Time-Domain Discrete- Wavelet-Transform Based Hybrid Detection of Series DC Arc Faults," in *IEEE Transactions on Power Electronics*, vol. 29, no. 6, pp. 3103-3115, June 2014.

[12] J. Johnson *et al*., "Photovoltaic DC Arc Fault Detector testing at Sandia National Laboratories," *2011 37th IEEE Photovoltaic Specialists Conference*, Seattle, WA, 2011, pp. 003614-003619.

[13] J. Johnson, S. Kuszmaul, W. Bower, et al. “Using PV module and line frequency response data to create robust arc fault detectors,” 2011.

[14] C. Luebke, T. Pier, B. Pahl, D. Breig and J. Zuercher, "Field test results of DC arc fault detection on residential and utility scale PV arrays," *2011 37th IEEE Photovoltaic Specialists Conference*, Seattle, WA, 2011, pp. 001832-001836.

[15] Y. J. Sun, Y. Gao, Y. D. Lin, et al. “dc fault arc detection method for photovoltaic systems using multiple criteria,” C.N. Patent 103245897A. 2013.

[16] L. Mu, Y. Wang, W. Jiang, et al. “Study on characteristics and detection method of DC arc fault for photovoltaic system,” in *Proceedings of the Csee*, 2016, vol. 36, no. 19.

[17] L. Cao. “Research on arc fault characteristics and detection technology in dc system,” in Nanjing University of Aeronautics and Astronautics, 2011.

[18] P. Sun, Z. Zheng, R. Yan, et al. “Detection method of arc fault in series with wavelet entropy,” in *Proceedings of the CSEE*, 2010.

[19] S. Zhang, F. Zhang, Z. Wang, et al. “Series arc fault identification method based on energy produced by wavelet transformation and neural network,” in *Transactions of China Electrotechnical Society*, 2014, pp.290-295 vol. 29, no. 6.

[20] Z. Wang and R. S. Balog, "Arc Fault and Flash Signal Analysis in DC Distribution Systems Using Wavelet Transformation," in *IEEE Transactions on Smart Grid*, vol. 6, no. 4, pp. 1955-1963, July 2015.

[21] W. Chen, Z. Wang, H. Xie and W. Yu, "Characterization of Surface EMG Signal Based on Fuzzy Entropy," in *IEEE Transactions on Neural Systems and Rehabilitation Engineering*, vol. 15, no. 2, pp. 266-272, June 2007.

[22] Costa, Madalena, A. L. Goldberger, and C. K. Peng. "Multiscale entropy analysis of biological signals. " *Physical Review E* vol. 71, no. 2, pp. 021906, 2005.

[23] J. Zheng, H. Pan, J. Cheng. “Rolling bearing fault detection and diagnosis based on composite multiscale fuzzy entropy and ensemble support vector machines,” *Mechanical Systems and Signal Processing*, vol. 85 pp:746-759, 2017.

[24] V. Cherkassky, "The Nature Of Statistical Learning Theory~," in *IEEE Transactions on Neural Networks*, vol. 8, no. 6, pp. 1564-1564, Nov. 1997.